Journal of Alloys and Compounds 495 (2010) 50–54

Contents lists available at ScienceDirect

Journal of Alloys and Compounds

journal homepage: www.elsevier.com/locate/jallcom

High temperature homogeneous plastic flow behavior of a Zr based bulk metallic glass matrix composite

Q. Wang[a,*], D.K. Wang[a], T. Fu[a], J.J. Blandin[b], J.M. Pelletier[c], Y.D. Dong[a]

[a] Institute of Materials Science, Shanghai University, 200072, People's Republic of China
[b] SIMAP-GPM2, CNRS, Grenoble-INP, UJF, BP 46, 38402 Saint-Martin d'Hères Cedex, France
[c] INSA de Lyon, MATEIS, Bât. B. Pascal, 69621 Villeurbanne Cedex, France

ARTICLE INFO

Article history:
Received 25 November 2009
Received in revised form 29 January 2010
Accepted 5 February 2010
Available online 12 February 2010

Keywords:
Metallic glass
Composite materials
Mechanical properties

ABSTRACT

In this paper, Zr based bulk metallic glass (BMG) composite consisting of nanocrystals embedded in the amorphous matrix was synthesized by controlled annealing treatment of a $Zr_{41.2}Ti_{13.8}Cu_{12.5}Ni_{10}Be_{22.5}$ amorphous alloy. The homogeneous plastic deformation behavior of the BMG composite was characterized in the supercooled liquid region, exhibiting non-Newtonian steady state plastic flow over the investigated strain rate domain. Based upon the analysis of rheological data in terms of a modified mechanistic model, it is revealed that the mechanism of the non-Newtonian plastic flow varies with temperature, which is closely related to the presence of nanocrystals within the glassy matrix.

1. Introduction

In the past decades, bulk metallic glasses (BMGs) have received increasing attention since they combine a high value of the yield stress with a particularly large elastic domain [1–3]. Moreover, the presence of a large supercooled liquid region (SLR) as well as a high thermal stability with respect to crystallization provides new opportunities for high temperature forming [4–6]. In order to improve the mechanical properties, particularly the ductility of BMGs suitable for structural applications, BMG composite materials have been developed by introducing nanocrystalline precipitates into a glassy matrix by controlled annealing treatment of amorphous precursors [7–10]. Extensive researches have been carried out on the room temperature mechanical properties of these composites, revealing good ductility and/or high strength [8–13]. Meanwhile, there have been a number of works concerned with the plastic flow behavior of the BMG composites at high temperatures, which is of importance for their workability [14–23]. In the previous investigations [15,17,18], the metallic glass matrix composites are found to exhibit large deformability in the SLR and their rheological behavior is usually explained in terms of the transition state theory [24,25]. Seemingly, the high temperature plastic deformation of the BMG composite is mainly controlled by viscous flow of the amorphous matrix.

However, the transition state theory is essentially thermomechanical, independent of the microstructure of the material [26]. The effect of crystalline phases on the plastic flow of the BMG composite is still unclear. Some questions are still open: (i) Do the crystals contribute directly to the deformation? (ii) Is the flow of the remaining glass constrained by the presence of crystals, thus modifying the viscous flow behavior? So, the mechanism of the high temperature deformation of BMG composites needs to be further investigated.

Among the multi-component BMGs, the $Zr_{41.2}Ti_{13.8}Cu_{12.5}Ni_{10}Be_{22.5}$ alloy (Vitreloy 1) is a particularly good glass former with a critical cooling rate as low as approximately 1 K/min [27]. This BMG exhibits a wide supercooled liquid region (SLR) and a high thermal stability against crystallization. Over the past years, a large number of experiments have been performed to study the effect of thermal treatment on the Zr based alloy by using a variety of techniques [28–36]. An interesting feature of this material is that the microstructure that is observed in the stage of primary crystallization is composed of nanocrystalline precipitates randomly embedded in the remaining amorphous matrix [28–31]. Moreover, it has been demonstrated that the composite microstructure has a high thermal stability against secondary crystallization during subsequent prolonged thermal exposure in SLR [29–31]. So, in the present work, the Zr based alloy subjected to primary nanocrystallization is chosen as the model material to study the steady state plastic flow of the BMG composite containing nanocrystals.

* Corresponding author at: Institute of Materials Science, Shanghai University, 269 P.O. Box, Yanchang Road 149, Shanghai University, Shanghai 200072, People's Republic of China.
E-mail address: qing-wang@hotmail.com (Q. Wang).

0925-8388/$ – see front matter © 2010 Elsevier B.V. All rights reserved.
doi:10.1016/j.jallcom.2010.02.017

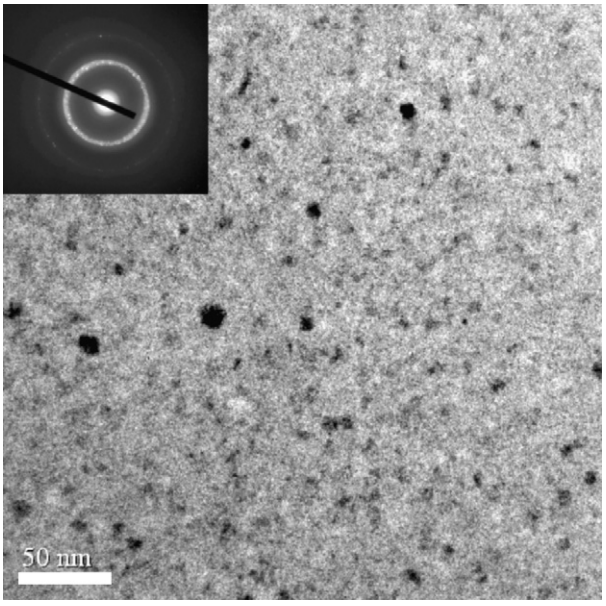

Fig. 1. A bright field TEM image of the $Zr_{41.2}Ti_{13.8}Cu_{12.5}Ni_{10}Be_{22.5}$ BMG annealed at 646 K for 2 h. The inset is the corresponding selected area electron diffraction pattern.

2. Experimental

The $Zr_{41.2}Ti_{13.8}Cu_{125}Ni_{10.0}Be_{22.5}$ (at.%) BMG alloy (Vitreloy 1) was supplied by Howmet Corp. (USA). The investigated BMG composite with nanocrystals dispersed in the amorphous matrix was prepared by isothermally annealing the as-received Zr based alloy at the temperature of 646 K (in the SLR) for 120 min. The thermal stability of the BMG composite was examined using a differential scanning calorimeter (Perkin-Elmer DSC7) at a heating rate of 10 K/min. Strain rate jump compression tests were carried out to study the rheological behavior of the BMG composite. For compression tests, cylindrical samples of 3 mm in diameter and 5 mm in height were used and both compressive sides were polished in order to be parallel. The samples were heated to a given testing temperature at the same rate of 10 K/min as used in DSC measurements and a maintaining of about 3 min was necessary to homogenize temperature before starting the mechanical test. The investigated temperature domain was from 646 to 675 K in the supercooled liquid region whereas the strain rate interval was from 2.5×10^{-4} to 2.5×10^{-3} s^{-1}. The microstructure of the BMG composite was investigated by a high resolution transmission electron microscope (HRTEM, JEOL 2010F) operated at 200 kV with a field-emission gun. The TEM specimens were prepared by the conventional method of slicing, grinding and then by the ion milling.

3. Results and discussion

Fig. 1 presents a typical bright field TEM micrograph of the $Zr_{41.2}Ti_{13.8}Cu_{125}Ni_{10.0}Be_{22.5}$ BMG annealed at the temperature of 646 K for 120 min. It is shown that the isothermal heat treatment leads to the precipitation of nanocrystals in the amorphous matrix. The size of the precipitates ranges from about 2 to 10 nm. The volume fraction of nanocrystals in the annealed Zr based BMG can be estimated to be about 10.5%, which is in agreement with that previously reported [37]. The corresponding selected area electronic diffraction pattern (SAED) consists of Bragg diffraction rings superimposed on the amorphous diffuse rings (see the inset of Fig. 1). The microstructure of the BMG composite is further confirmed by using HRTEM. It is revealed in Fig. 2(a) and (b) that the investigated BMG composite is composed of nanocrystals surrounded by the amorphous matrix, revealing a typical characteristic of lattice fringe. The Fourier transfer (FT) treatments on the selected area of the HRTEM image were performed, as shown in the insets of Fig. 2(a) and (b). Apparently, the diffraction spots from the nanocrystal can be seen.

Fig. 3 shows a comparison of DSC traces for the as-received and partially nanocrystallized BMG at a heating rate of 10 K/min. The as-received sample exhibits a distinct endothermic characteristic due to glass transition and three exothermic peaks upon the crystallization of the supercooled liquid phase at high temperatures. For the as-received alloy, the T_g, T_x and $\Delta T_x = T_x - T_g$ (defined as supercooled liquid region) are 619, 698, and 79 K, respectively. After isothermally annealing at 646 K for 120 min, the T_g and T_x are enhanced to be 627 and 721 K, respectively, leading to a broadened supercooled liquid region of 94 K, while the first exothermic peak corresponding to the primary crystallization vanishes. The shift of glass transition towards to higher temperature as well as the presence of widened supercooled liquid region for the pre-annealed sample indicates that the thermal stability against crystallization of the remaining supercooled metallic liquid are higher than that of the initial homogeneous amorphous phase. This might offer us an opportunity to investigate the steady state plastic flow of BMG matrix composites reinforced with nanocrystals at high temperatures.

Fig. 4 shows a typical true stress versus true strain curve obtained by strain rate jump compression test at the temperature of 665 K. Whatever the strain rate, a constant flow stress is quickly reached, revealing a steady state plastic flow. When the testing temperature is decreased (e.g. $T = 655$ K), stress overshoots are detected whereas they disappear for a higher temperature (e.g. $T = 675$ K). Similar phenomena have been observed for the monolithic Zr based BMGs in the SLR [38]. It is worth noting that no conspicuous strain hardening was observed whatever the testing temperature, suggesting that no significant microstructural modification, e.g. the secondary crystallization of the remaining amorphous matrix occurred during the compression tests at the given temperatures [16].

Using experimental data from the strain rate jump tests, the double logarithmic plots of strain rate versus stress for various testing temperatures were performed, as shown in Fig. 5. It is illustrated that the flow stress is dependent on both strain rate and testing temperature. At temperatures between 646 and 675 K, the flow stress of the BMG composite increases with increasing strain rate over the investigated domain from 2.5×10^{-4} to 5×10^{-3} s^{-1}. Moreover, the calculated value of strain rate sensitivity parameter m ($= \Delta \log \sigma / \Delta \log \dot{\varepsilon}$) is much less than unity, varying from 0.15 to 0.55. This indicates a non-Newtonian type of viscous flow. Note that the strain rate sensitivity m varies with not only strain rate but also testing temperature. For example, at a given temperature of 646 K, the value of m decreases with increasing strain rate from 0.25 at 2.5×10^{-4} s^{-1} to 0.15 at 2.5×10^{-3} s^{-1}. However, at a given strain rate of 2.5×10^{-4} s^{-1}, it rises from 0.25 up to 0.55 when the testing temperature is elevated from 646 to 675 K.

It has been demonstrated in previous investigations [15,17,18] that the plastic flow behavior of the BMG composite reinforced with a second crystalline phase could be described by the transition state theory derived from free volume model [24,25], which predicts a strain rate-stress relation in the form:

$$\dot{\varepsilon} = \dot{\varepsilon}_0 \sinh\left(\frac{\sigma V_{act}}{2\sqrt{3}kT}\right) \quad (1)$$

where k is the Boltzmann's constant and T is the temperature, and the activated volume, V_{act} as well as the reference strain rate $\dot{\varepsilon}_0$ are used as fitting parameters for adapting calculated curves to the experimental data. Nevertheless, we note that the logarithm strain rate versus logarithm stress curves of the investigated BMG composite cannot be fitted by using Eq. (1) with the least-square method except for the lowest testing temperature of 646 K (see Fig. 5). This suggests that the effect of nanocrystals on the viscous flow of the amorphous matrix cannot be ignored and different mechanisms of plastic deformation might come into effect at higher temperatures in the studied BMG composite.

In order to account for the rheological behavior of the BMG composite at high temperatures, one may alternatively consider

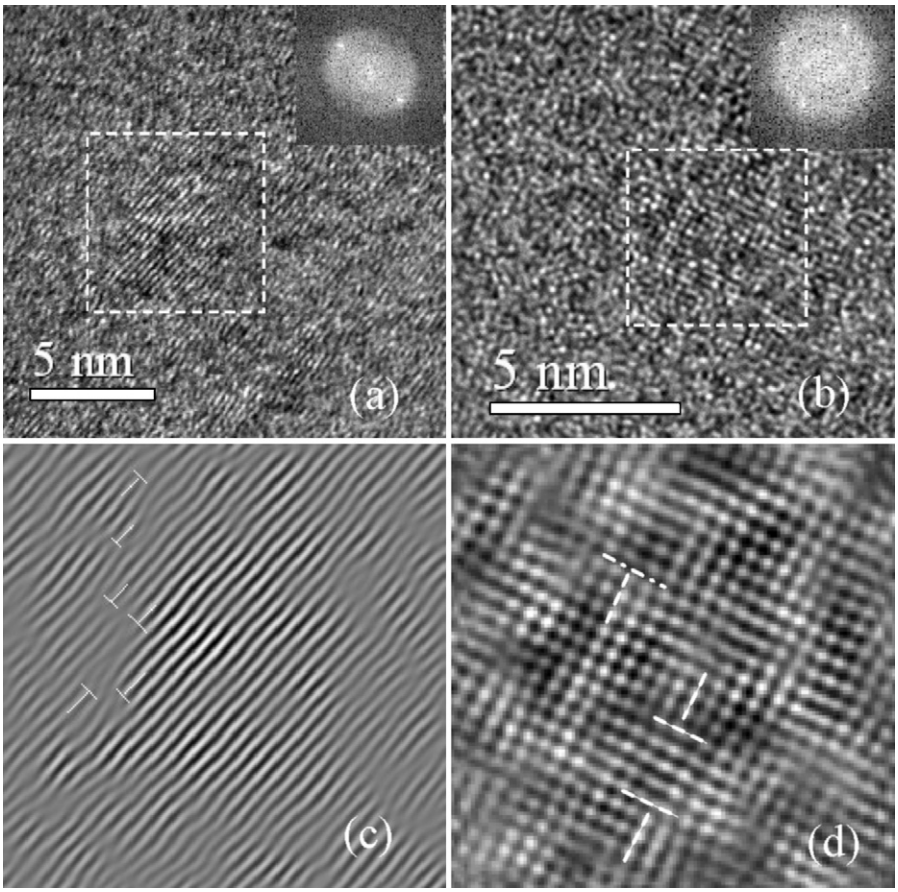

Fig. 2. HRTEM images (a) and (b) showing a nanocrystal embedded in the amorphous matrix of the BMG composite; inset: the Fourier transfer pattern of the selected area; (c) and (d) the corresponding inverse Fourier transfer (IFT) images.

a mechanistic model [39]. From a rheological viewpoint, the shear rate of a glass, $\dot{\gamma}$, is a nonlinear function of applied shear stress, τ, and can mathematically be expanded into a Taylor series:

$$\dot{\gamma} = f(\tau) = \sum_{i=1}^{n} A_i \tau^i = A_1\tau + A_2\tau^2 + A_3\tau^3 + A_4\tau^4 + A_5\tau^5 + \cdots + A_n\tau^n \quad (2)$$

Note that each term in the above series corresponds to a particular physical mechanism and that the respective order of Eq. (2) is not universal but has to be determined for the alloy system, the testing temperature, strain rate and the microstructure of the material. In a first approximation, the total deformation rate for nanocrystalline/amorphous mixture can be expressed by:

$$\dot{\gamma}_{total} = (1 - f_v)\dot{\gamma}_{am} + f_v\dot{\gamma}_{cry} \quad (3)$$

where $\dot{\gamma}_{total}$ is the total strain rate, $\dot{\gamma}_{am}$ and $\dot{\gamma}_{cry}$ is the strain rate of the amorphous and crystalline phase, respectively, and f_v is the volume fraction of crystalline phase. Since the plastic flow of an amorphous alloy can be described by $\dot{\gamma}_{am} = A\tau$, and the plastic flow

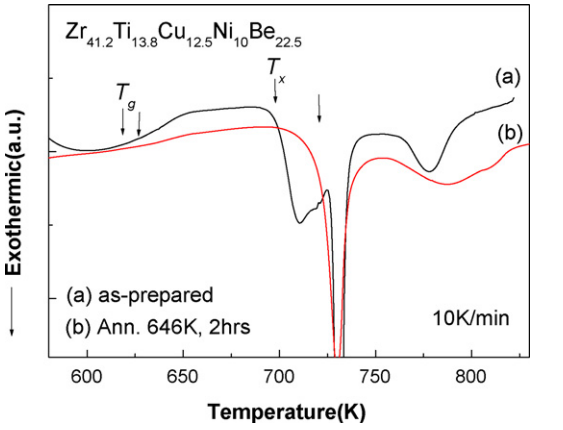

Fig. 3. DSC curves obtained at a heating rate of 10 K/min for the as-received sample (a) and the sample annealed at 646 K for 2 h (b).

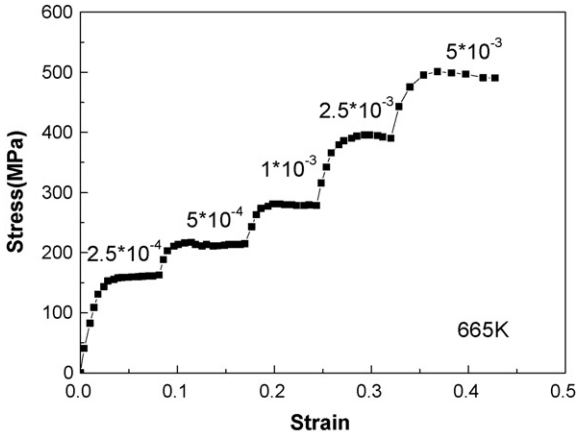

Fig. 4. A typical true stress versus true strain curve showing the effect of strain rate during the compressive deformation at 665 K for the BMG composite.

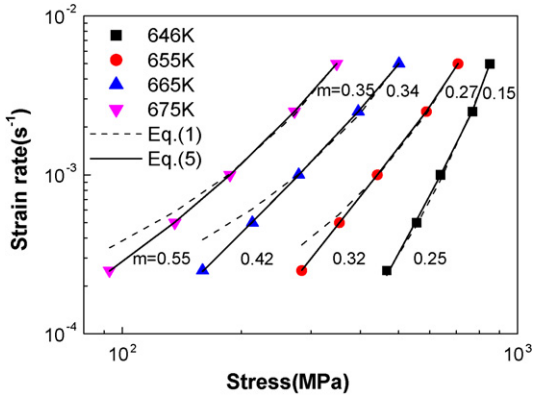

Fig. 5. Strain rate–stress relations at various temperatures for the BMG composite and fits to experimental data using the functions as described in the text.

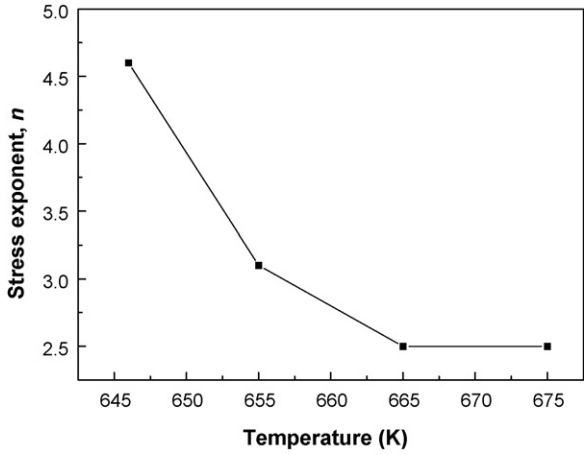

Fig. 6. Temperature variation of the stress exponent *n*.

of a nanocrystalline alloy can be described by $\dot{\gamma}_{cry} = B\tau^n$, the total deformation rate in the alloy composed of nanocrystalline grains embedded in the amorphous matrix is simply expressed by

$$\dot{\gamma}_{total} = (1 - f_v)A\tau + f_v B\tau^n \quad (4)$$

where τ is the flow stress, n the stress exponent ($n \geq 2$), A and B are material constants.

As the mechanical model suggested, the measured strain rate sensitivity parameter would have to fall between 0.5, i.e. $n = 2$, the value for grain boundary sliding in fine-grained crystalline material, and unity, the value for Newtonian viscous flow if a mixed nanocrystalline-plus-amorphous structure contains aggregates of nanocrystalline grains. However, if an alloy contains isolated nanocrystalline grains in an amorphous matrix, the overall strain rate sensitivity parameter would be less than unity, i.e. $n > 1$ but is not bounded at a lower level by $m = 0.5$ [26,39].

Indeed, the high temperature plastic flow behavior of the investigated BMG composite can be described by using the above mechanical model. The m value of the composite falls between 0.15 and 0.55, without bounding at a lower level by $m = 0.5$ (see Fig. 5) while the HRTEM/TEM observations demonstrate that the microstructure of the composite material is composed of the isolated nanocrystals within the amorphous matrix (see Fig. 2).

Nevertheless, taking into account that the response of the composite including the amorphous matrix and reinforcements could be nonlinear [20,40], we may write a modified form of Eq. (4) as

$$\dot{\gamma}_{total} = (1 - f_v)^d A \sinh\left(\frac{\tau V_{act}}{2kT}\right) + f_v B\tau^n \quad (5)$$

In the present case, where m ranges from 0.15 to 0.55, the appropriate values of exponent, d lie in the range ~3–5 [40].

Interestingly, it is revealed in Fig. 5 that the strain rate versus flow stress data points are well fitted by using Eq. (5), yielding the value of the stress exponent, n for each testing temperature. The temperature dependence of n for the BMG composite is shown in Fig. 6. The value of n is found to decrease from 4.6 down to 2.5 as the testing temperature is raised from 646 up to 665 K. Above 665 K, the stress exponent tends to be independent of temperature. Therefore, it is indicated that the mechanism of viscous flow in the studied BMG composite varies with the testing temperature. According to the above model, the BMG composite can be considered as a dispersion-strengthened solid at a relatively low temperature, e.g. 646 K, since the value of n is close to 5, which agrees with HRTEM/TEM observations. However, the stress exponent of 2.5 obtained at temperatures higher than 665 K means that a different plastic deformation mechanism could operate in the crystalline lattice [39]. As a consequence, it is worthwhile to investigate the microstructure of the precipitated nanocrystallites and its effect on the high temperature plastic flow behavior of the BMG composite. To characterize the detailed microstructure of the nanoparticle, the inverse Fourier transfer (IFT) treatments on the selected local area of the corresponding HRTEM image have been performed, as shown in Fig. 2(c) and (d). It is interesting to note that the dislocations are seen in the precipitated nanocrystal in accompany with the presence of lattice distortion. This may be the reason why the rheological behavior of the Zr based BMG matrix composite could be modified at higher temperatures.

4. Conclusions

The Zr based BMG composite with nanocrystals embedded in the amorphous matrix was synthesized after primary nanocrystallization of a $Zr_{41.2}Ti_{13.8}Cu_{12.5}Ni_{10}Be_{22.5}$ glassy alloy. The rheological behavior of the BMG matrix composite in the supercooled liquid region can be well described by a modified mechanical model. It is revealed that the mechanism of the non-Newtonian steady state plastic flow varies with temperature, which is closely related to the presence of nanocrystals in the amorphous matrix.

Acknowledgements

The authors are grateful to the financial support of the Natural Science Foundation of China (Grant No: 50871063, 50731008), and the ARCUS program between France and China.

References

[1] A. Inoue, Acta Mater. 48 (2000) 279–306.
[2] Z.F. Zhang, J. Eckert, L. Schultz, Acta Mater. 51 (2003) 1167–1179.
[3] A.R. Yavari, J.J. Lewandowski, J. Eckert, MRS Bull. 32 (2007) 635–638.
[4] K.S. Lee, T.K. Ha, S. Ahn, Y.W. Chang, J. Non-Cryst. Solids 317 (2003) 193–199.
[5] J.P. Chu, C.L. Chiang, T. Mahalingam, T.G. Nieh, Scripta Mater. 49 (2003) 435–440.
[6] A. Inoue, N. Nishiyama, MRS Bull. 32 (2007) 651–658.
[7] A. Leonhard, L.Q. Xing, M. Heilmaier, A. Gebert, J. Eckert, L. Schultz, Nanostruct. Mater. 10 (1998) 805–817.
[8] C. Fan, A. Takeuchi, A. Inoue, Mater. Trans. JIM 40 (1999) 42–51.
[9] K. Mondal, T. Ohkubo, T. Toyama, Y. Nagai, M. Hasegawa, K. Hono, Acta Mater. 56 (2008) 5329–5339.
[10] J. Eckert, J. Das, S. Pauly, C. Duhamel, J. Mater. Res. 22 (2007) 285–301.
[11] C. Fan, C. Li, A. Inoue, V. Haas, Phys. Rev. B 61 (2000) R3761–3763.
[12] R. Doglione, S. Spriano, L. Battezzati, Nanostruct. Mater. 8 (1997) 447–456.
[13] L.Q. Xing, J. Eckert, W. Löser, L. Schultz, Appl. Phys. Lett. 74 (1999) 664–666.
[14] D.H. Bae, J.M. Park, J.H. Na, D.H. Kim, Y.C. Kim, J.K. Lee, J. Mater. Res. 19 (2004) 937–942.
[15] X.L. Fu, Y. Li, C.A. Schuh, Appl. Phys. Lett. 87 (2005) 2419041–2419043.
[16] M. Bletry, P. Guyot, Y. Brechet, J.J. Blandin, J.L. Soubeyroux, Intermetallics 12 (2004) 1051–1055.

[17] A. Reger-Leonhard, M. Heilmaier, J. Eckert, Scripta Mater. 43 (2003) 459–464.
[18] K.C. Chan, Q. Chen, L. Liu, Intermetallics 15 (2007) 500–505.
[19] X.L. Fu, Y. Li, C.A. Schuh, J. Mater. Res. 22 (2007) 1564–1573.
[20] X.L. Fu, Y. Li, C.A. Schuh, Acta Mater. 55 (2007) 3059–3071.
[21] S. Gravier, J.J. Blandin, P. Donnadieu, Phil. Mag. 88 (2008) 2357–2372.
[22] H.J. Jun, K.S. Lee, C.P. Kim, Y.W. Chang, Metals Mater. Int. 14 (2008) 297–306.
[23] H.J. Jun, K.S. Lee, U. Kuhn, J. Eckert, Y.W. Chang, Mater. Sci. Eng. A 526 (2009) 62–68.
[24] A.I. Taub, Acta Metall. 28 (1980) 633–637.
[25] A.I. Taub, F.E. Luborsky, Acta Metall. 29 (1981) 1939–1948.
[26] T.G. Nieh, J. Wadsworth, Scripta Mater. 54 (2006) 387–392.
[27] A. Peker, W.L. Johnson, Appl. Phys. Lett. 63 (1993) 2342–2344.
[28] S. Schneider, P. Thiyagarajan, W.L. Johnson, Appl. Phys. Lett. 68 (1996) 493–495.
[29] M.-P. Macht, N. Wanderka, A. Wiedenmann, H. Wollenberger, Q. Wei, H.J. Fecht, S.G. Klose, Mater. Sci. Forum 225–227 (1996) 65–70.
[30] A. Wiedenmann, U. Keiderling, M.-P. Macht, H. Wollenberger, Mater. Sci. Forum 225–227 (1996) 71–76.
[31] N. Wanderka, Q. Wei, R. Doole, M. Jenkins, S. Friedrich, M.-P. Macht, H. Wollenberger, Mater. Sci. Forum 269–272 (1998) 773–778.
[32] M.K. Miller, Mater. Sci. Eng. A 250 (1998) 133–140.
[33] N. Wanderka, U. Czubayko, P. Schubert-Bischoff, M.-P. Macht, Mater. Sci. Eng. A 270 (1999) 44–47.
[34] J.F. Löffer, W.L. Johnson, Appl. Phys. Lett. 76 (2000) 3394–3396.
[35] X.-P. Tang, J.F. Löffer, W.L. Johnson, Y. Wu, J. Non-Cryst. Solids 317 (2003) 118–122.
[36] I. Martin, T. Ohkubo, M. Ohnuma, B. Deconihout, K. Hono, Acta Mater. 52 (2004) 4427–4435.
[37] T.A. Waniuk, R. Busch, A. Masuhr, W.L. Johnson, Acta Mater. 46 (1998) 5229–5236.
[38] Q. Wang, J.M. Pelletier, J.J. Blandin, M. Suery, J. Non-Cryst. Solids 351 (2005) 2224–2231.
[39] T.G. Nieh, J. Wadsworth, C.T. Liu, T. Ohkubo, Y. Hirotsu, Acta Mater. 49 (2001) 2887–2896.
[40] B.I. Lee, M.E. Mear, J. Mech. Phys. Solids 39 (1991) 627–649.